Biochemistry

Article

Cite This: Biochemistry 2018, 57, 6404−6415

pubs.acs.org/biochemistry

Spontaneous Calcium-Independent Dimerization of the Isolated First Domain of Neural Cadherin

Samantha Davila,[†] Peilu Liu,[‡,§] Alexis Smith,[†,∥] Alan G. Marshall,[‡,§] and Susan Pedigo*[,†]

[†]Department of Chemistry and Biochemistry, University of Mississippi, University, Mississippi 38677, United States

[‡]Department of Chemistry & Biochemistry, Florida State University, Tallahassee, Florida 32306, United States

[§]Ion Cyclotron Resonance Program, National High Magnetic Field Laboratory, Florida State University, Tallahassee, Florida 32310, United States

Supporting Information

ABSTRACT: Cadherins are calcium-dependent, transmembrane adhesion molecules that assemble through direct noncovalent association of their N-terminal extracellular modular domains. As the transmembrane component of adherens junctions, they indirectly link adherent cells' actin cytoskeletons. Here, we investigate the most distal extracellular domain of neural cadherin (N-cadherin), a protein required at excitatory synapses, the site of long-term potentiation. This domain is the site of the adhesive interface, and it forms a dimer spontaneously without binding calcium, a surprising finding given that calcium binding is required for proper physiological function. A critical tryptophan at position 2, W2, provides a spectroscopic probe for the "closed" monomer and strand-swapped dimer. Spectroscopic studies show that W2 remains docked in the two forms but has a different apparent interaction with the hydrophobic pocket. Size-exclusion chromatography was used to measure the levels of the monomer and dimer over time to study the kinetics and equilibria of the unexpected spontaneous dimer formation (K_d = 130 μM; τ = 2 days at 4 °C). Our results support the idea that NCAD1 is missing critical contacts that facilitate the rapid exchange of the βA-strand. Furthermore, the monomer and dimer have equivalent and exceptionally high intrinsic stability for a 99-residue Ig-like domain with no internal disulfides (T_m = 77 °C; ΔH = 85 kcal/mol). Ultimately, a complete analysis of synapse dynamics requires characterization of the kinetics and equilibria of N-cadherin. The studies reported here take a reductionist approach to understanding the essential biophysics of an atypical Ig-like domain that is the site of the adhesive interface of N-cadherin.

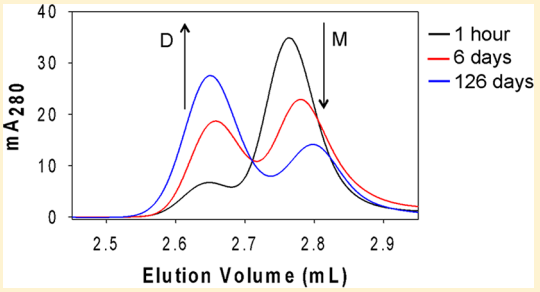

Classical cadherins are transmembrane glycoproteins that are the adhesive component of adherens junctions. Cadherins mediate communication between adherent cells in normal, stable tissues of vertebrate and invertebrate animals by linking the actin cytoskeletons of adjacent cells. They are vital in biological functions that are dependent on proper cell adhesion, including regulation of cell signaling,[1,2] tissue morphogenesis,[3] synaptogenesis,[4] synapse maintenance,[5] and the regulation of synaptic plasticity.[6−8] Knowledge of the molecular basis for cadherin-mediated cell−cell adhesion is crucial for understanding physiology as well as addressing abnormalities in adhesion. The studies reported here address unusual properties of NCAD1, the most distal extracellular domain of neural cadherin (N-cadherin), which contains the adhesive interface. N-Cadherin is critical for diverse processes such as adhesion between pre- and postsynaptic cells in neurological synapses[9−13] and between endothelial cells in developing vasculature.[14,15] Furthermore, it is also an integral component of metastatic cancer in that abnormal expression in carcinoma leads to the establishment of colonies of transformed cells at secondary sites.[16,17] Given the diversity of these venues, an understanding of the intrinsic properties of NCAD1 is essential.

Classical cadherins have a common domain organization that includes an extracellular (EC) region, a single-pass transmembrane region, and a conserved C-terminal cytoplasmic region. The EC region has five seven-stranded antiparallel β-barrel, Ig-like domains that are approximately 100 amino acids each and are denoted as EC1−EC5 starting from the N-terminus. Between domains, seven-residue linker segments create interdomain interfaces where three calcium ions bind. Studies commonly focus on the two-domain construct [EC1−linker 1−EC2; EC12 (Figure 1A)] because it is the minimal functional subunit that is able to fold properly, bind calcium, and dimerize. A wide range of studies, including cell aggregation,[3,18] bead aggregation,[19] force measurements,[20] and cell cultures,[21] have established calcium binding as a requirement for the adhesive dimerization of classical cadherins. The binding of calcium drives dimerization by inducing strain in the calcium-saturated monomer. Strain is relieved upon formation of a strand-swapped dimer.[22]

Received: July 7, 2018
Revised: October 2, 2018
Published: November 2, 2018

DOI: 10.1021/acs.biochem.8b00733
Biochemistry 2018, 57, 6404−6415

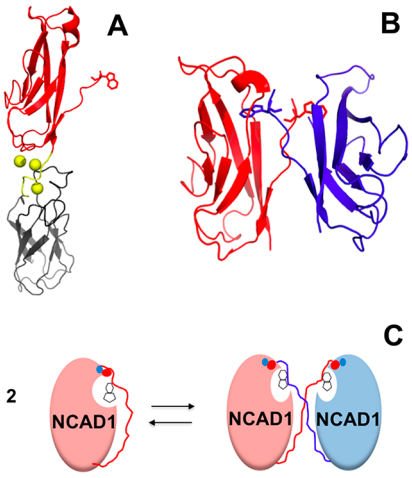

Figure 1. Ribbon drawings and schematic representations of strand-swapped dimers. (A) Ribbon drawing of NCAD12, EC1 (red), linker 1 and calcium spheres (yellow), and EC2 (gray). The βA-strand is "open" because it is docked in a partner protomer that is not shown (PDB entry 2QVI;[23] Pymol[24]). (B) Ribbon drawing of the NCAD1 dimer (PDB entry 1NCI[25]). The swapped βA-strands are apparent. W2 is docked into a hydrophobic pocket of the partner protomer. The W2 side chains are illustrated as sticks. (C) Schematic representation of the "closed" monomers that interact to form the strand-swapped dimer. The ionic interaction between the positively charged N-terminus (red circle) and the side chain of E89 (blue circle) is shown.

Studies in this work focus on the unusual properties of the isolated EC1 domain in N-cadherin [NCAD1 (Figure 1B)]. NCAD1 is unable to bind calcium because it is missing the calcium-binding residues from the EC2 domain and linker region. Despite the lack of the essential components for calcium binding, NCAD1 forms a dimer spontaneously, a finding that deviates from the dimerization paradigm for the classical cadherin family and is unusual for isolated Ig-like domains. All studies included in this work focus on the biophysics of stable dimer formation by NCAD1 and aim to address two major questions: (1) What structural components are responsible for the remarkable stability of NCAD1? (2) Why does NCAD1 spontaneously form a dimer in the absence of binding of calcium?

Structural and functional characteristics of classical cadherins are understood to depend critically upon calcium binding. As briefly mentioned, binding of calcium to the linker regions between successive domains rigidifies the molecule and induces strain in the monomer. The strand-swapped dimer forms between the N-terminal EC1 domains of the adhesive partners by swapping the N-terminal βA-strands, docking tryptophan 2 (W2) in the adherent protomer's hydrophobic pocket, and forming an ionic interaction between the positively charged N-terminus and the side chain of E89 (Figure 1C). These same critical noncovalent interactions in the "closed" monomer re-form in the dimer. The E89A mutation causes a red-shift in the fluorescence emission spectrum, implying that W2 is more exposed if the ionic interaction is not present.[22] In addition, the W2A mutation abrogates strand-swapped dimerization.[22,26,27]

Named for the tissue type in which they predominate, epithelial and neural cadherins are among the best studied in the field. Although 81% of the primary structure is considered "similar", ECAD and NCAD are found in distinct locations and have significantly different calcium-responsive properties. Biophysical studies of site-directed mutants have attempted to explain the forces that stabilize strand-swapped dimers of these classical cadherins, and fundamental questions regarding the striking differences between them arise. ECAD12 dimers display fast exchange between monomer and dimer states, regardless of the calcium concentration.[28] Current models attribute these rapid exchange kinetics to the formation of an initial encounter "X dimer" complex, a transient intermediate that functions as the transition state between the closed monomer and the strand-swapped dimer.[29] In contrast, the kinetics of monomer−dimer exchange in NCAD12 depend strongly on the calcium concentration. For NCAD12, monomer−dimer exchange is rapid only in the presence of calcium, pointing to the existence of (or access to) an initial encounter complex only in the calcium-saturated state.[28] However, the X-dimer intermediate established in ECAD12 is not present, as such, in NCAD12. Specifically, the critical requirement of X-dimer residue K14 for rapid dimerization kinetics in ECAD12 is not recapitulated in NCAD12.[30] Moreover, the NCAD12 calcium-saturated dimer (D_{sat}) species can form a kinetically trapped dimer (D^*_{apo}) through decalcification of calcium-saturated NCAD12 stocks with EDTA (cf. Jungles et al.[31]). This drastic change in kinetics upon decalcification again points to the existence of an initial encounter complex in NCAD12 that is not accessible in the absence of calcium or the existence of an altogether different interface that is accessible.

The unique ability of NCAD1 to spontaneously form a dimer provides insight into an interesting protein folding/function question of particular relevance to the dynamics of excitatory synapses. Here we define the minimal unit that can form a dimer without binding calcium and determine the kinetics and equilibria of this phenomenon. These studies serve as an end point in the discussion of synapse plasticity at extreme low calcium levels. We present the results of systematic studies of the structure and function of NCAD1 that (1) monitor differences in the environment of W2 in the monomeric and dimeric forms of NCAD1, (2) measure the assembly and disassembly constants for this unusual dimerization phenomenon as well as an equilibrium constant for NCAD1 in the absence of calcium, and (3) define a very stable core structure regardless of the dimerization state. Our results indicate that N-cadherin forms significant levels of slow-exchange dimer without the calcium binding driving force. These findings are consistent with N-cadherin's ability to adapt the kinetics and equilibria of adhesive phenomena in response to a fluctuating calcium concentration.

MATERIALS AND METHODS

Protein Cloning, Expression, and Purification. Recombinant plasmid construction and cloning of the gene for the first two extracellular domains (residues 1−221; EC12) of N-cadherin have been previously described in detail.[28] For this work, the isolated first domain construct NCAD1 (residues 1−99; EC1) was created by introducing a stop codon at the end of the EC1 coding region by site-directed mutagenesis of the NCAD12/WT plasmid. The mutation was confirmed by sequencing of the plasmid. The protein was overexpressed and purified from bacterial inclusion bodies by use of denaturing HisTag chromatography following a previously established protocol.[28] The purity and size of the protein were assessed with 17% reducing, denaturing polyacrylamide gels as well as mass spectrometry. Apo-NCAD1 stocks were prepared by

DOI: 10.1021/acs.biochem.8b00733
Biochemistry 2018, 57, 6404−6415

extensive dialysis in 10 mM HEPES and 140 mM NaCl (pH 7.4). The contaminating calcium concentration was determined to be 1 μM by atomic adsorption spectroscopy. The concentration of the stock was determined spectrophotometrically with a Cary 50 Bio ultraviolet−visible (UV−vis) spectrophotometer by use of a 1 cm quartz cuvette with an extinction coefficient at 280 nm of 6970 ± 200 M^{-1} cm^{-1} determined experimentally.[32]

Preparation of Monomeric and Dimeric NCAD1 Stocks. To study the kinetics and equilibria of dimerization as well as unique spectroscopic signals, we prepared monomer- and dimer-enriched samples. At every stage of preparation, we assessed the relative proportion of the monomer and dimer in the NCAD1 stocks by use of analytical size-exclusion chromatography (SEC), as described below. Throughout this work, we refer to the dimer concentration or percent dimer (% D) in terms of the total protein concentration, $[M]_o$, and free monomer concentration, [M], such that $[M]_o = [M] + [D]$. The initial concentration of the dimer immediately following protein preparation (initial stock) was lower than that of the monomer (<35% D). Over a period of several months at −20 °C, the dimer concentration in the stock increased such that >70% of the total protein concentration was in the form of a dimer. This dimer-enriched NCAD1 stock was heated in water baths at varying temperatures for various time periods. Heating at 50 °C for a total of 10 min showed maximum disassembly of the dimer without precipitation of the protein. This "heat treatment" reversibly converted the dimer to its monomeric form and became the working monomeric stock (<15% D). Henceforth, the NCAD1 stock with a high level of dimer and a high level of monomer will be termed the dimer and monomer stocks. Details of dimer levels for each experiment are noted in the figure legends.

Analytical Size-Exclusion Chromatography (SEC). Analytical size-exclusion chromatography (SEC) was used to determine the relative ratio of monomeric and dimeric species in solution. Over the duration of the experiments reported here, two systems were employed. Experiments were performed by using an ÄKTA Purifier high-performance liquid chromatography (HPLC) instrument (GE Life Sciences) with a Superose-12 10/300 GL column (GE Life Sciences) with detection at 280 nm and a flow rate of 0.5 mL/min. The total column volume was approximately 25 mL, and approximately 50 μL of protein was loaded onto the column. SEC experiments were also performed with a ZORBAX GF-250 analytical column (4.6 mm × 250 mm, 4 Micron, Agilent) by using an Agilent 1100 HPLC Chemstation with UV−vis absorbance detection at 280 nm with a flow rate of 1 mL/min. The total column volume was approximately 5 mL, and 5 μL of protein was loaded onto the column. All studies were conducted in apo mobile phases [140 mM NaCl and 10 mM HEPES (pH 7.4)] at room temperature. Columns were previously calibrated with Bio-Rad Gel Filtration Standard Mix. Because of their oblong shape, all cadherins appear to be larger in SEC than predicted on the basis of their molecular weight.[33] The concentrations of the monomer and dimer for NCAD1 stocks were calculated on the basis of fractional peak heights. Identical estimates of monomer and dimer concentrations were obtained from fractional peak areas.

Spectroscopic Studies of Structural Differences in the Monomer and Dimer. Circular dichroism signals of NCAD1 stocks were monitored by use of an AVIV 202SF circular dichroism spectrometer with CDS 3.02A software made by AVIV Biomedical, Inc. Cadherin's secondary structures, mostly β-sheets, have a recognized negative signal with a minimum at approximately 218 nm.[34] High-concentration NCAD1 samples gave spectra with the best signal-to-noise with a 0.5 mm path length quartz cuvette. Scans were acquired from 300 to 200 nm in 1 nm increments with 5 s averaging time, and the temperature of the jacket was held constant at 25 °C.

The intrinsic tryptophan fluorescence emission for each of the NCAD1 stocks was evaluated by using a Photon Technology International (PTI) fluorescence spectrometer equipped with an A1010B arc lamp and Felix 3.2 software. Excitation was set at 292 nm, which is the optimum excitation for tryptophan that minimizes direct excitation of tyrosine. Emission was measured at wavelengths ranging from 300 to 420 nm. The scan step size was set to 1 nm, and the integration and averaging time to 1 s with the emission polarizer angle at 54.7°. All scans were made at 25 °C with stirred 2.5 μM protein solutions in a 1 cm path length quartz cuvette.

Equilibrium and Kinetic Studies of Calcium-Independent Dimerization of NCAD1. *Dimer Assembly.* To determine the rate of dimer formation as a function of time, a heat-treated NCAD1 monomer stock (140 μM) and a dilution (70 μM) were injected onto the SEC column at various times ranging from 60 min to 4 months.

Dimer Disassembly. To determine the rate of dimer disassembly as a function of time, a dimer NCAD1 stock (140 μM) and its dilution (70 μM) were studied. Both concentrations were injected onto the SEC column at various times ranging from 60 min to 1 month.

Data Analysis. Chromatographic data were analyzed on the basis of a reversible bimolecular binding reaction (eq 1) by using custom scripts written with IGOR Pro software and verified by simulated data constructed with Microsoft Excel.

$$\mathrm{M} + \mathrm{M} \rightarrow \mathrm{D};\ K_d = \frac{[M]^2}{[D]} \tag{1}$$

The second-order assembly data were analyzed by the following equations to yield an observed association constant, k_{obs}, given by eqs 2 and 3, in which the fraction of dimer, f_D, is a function of the total protein concentration, $[M]_o$, and the free monomer concentration, [M]. We corrected the level of $[M]_o$ in the association reaction to reflect residual dimer post-heat treatment.

$$f_D = \frac{[M]_o - [M]}{[M]_o};\ [M] = 1/\left(\frac{1}{[M]_o} + k_{obs}t\right) \tag{2}$$

$$\text{span} = [M]_o - [M]_{plateau};$$

$$[M]_{plateau} = \left(-K_d + \sqrt{{K_d}^2 + 8K_d[M]_o}\right)/4 \tag{3}$$

The concentration of the dimer at the plateau was determined from the initial concentration of the protein, $[M]_o$, and the equilibrium dissociation constant, K_d.

The rate of the first-order dissociation reaction and the equilibrium dissociation constant were derived from eq 4.

$$\text{rate} = k_r[D];\ f_D = e^{-k_r t} \tag{4}$$

The time constant for the dissociation reaction, $t_{1/2}$ (or τ), is given by eq 5 and is the time required for half of the dimers to

DOI: 10.1021/acs.biochem.8b00733
Biochemistry 2018, 57, 6404−6415

dissociate. Again, at the plateau, the concentration of the dimer was determined from K_d as given by eq 3.

$$t_{1/2} = \frac{0.693}{k_r} \quad (5)$$

Stability Studies of the NCAD1 Monomer and Dimer. Thermal unfolding for each of the stocks was monitored by CD spectroscopy performed with a 1 cm quartz cuvette with a screwtop temperature probe. The temperature ramp rate was 1 °C/min with a 30 s to 1 min equilibration at each temperature before a 5 s acquisition time at a fixed wavelength of 227 nm with stirring. The temperature ranged from 15 to 90 °C, and the reversibility for each of the transitions was recorded from cooling scans done immediately following heating scans. Data were analyzed by fitting data to the Gibbs−Helmholtz equation by using custom scripts (IGOR Pro software and Microsoft Excel) as reported previously.[35] Parameters were resolved from linear native and denatured baselines with adjustable slopes and intercepts. The value of ΔC_p was fixed at 1 kcal mol^{-1} K^{-1} to resolve values for ΔH_m and T_m. The sensitivity of the resolved parameters to ΔC_p was tested by fixing ΔC_p to 0, 1, 2, or 3 kcal mol^{-1} K^{-1}; the changes in resolved parameters were within the standard deviations in the best-fit values found by fixing ΔC_p to 1 kcal mol^{-1} K^{-1}.

We utilized the program GetArea[36] to estimate the solvent-accessible surface area based on the published crystallographic structure of PDB entry 1NCI.[26] We determined the solvent exposure of amino acid side chains to aqueous buffer in terms of the percentage of the side chain accessible to water (0.14 nm diameter).

Proteolytic mapping of NCAD1 with Protease XIII was performed at the National High Magnetic Field Laboratory in Tallahassee, FL, to determine sequence coverage for hydrogen/deuterium-exchange mass spectrometry (HDX-MS) experiments. The proteolytic susceptibility to Protease XIII was determined for samples of the NCAD1 dimer and monomer, freshly heat-treated to ensure that the protein was in its monomeric form. A 5 μL volume of the protein sample was diluted in 45 μL of 140 mM NaCl and 10 mM HEPES buffer (pH 7.4). The protein was then denatured with 8 M urea and 200 mM TCEP in a 1% formic acid solution at pH 2.5 and then digested for approximately 3 min at 0.4 °C with 60% saturated Protease XIII (Sigma-Aldrich, St. Louis, MO). The peptides from the digest were separated and desalted by HPLC (Jasco HPLC/SFC). A rapid gradient from 2 to 95% B [A, 5/95/0.5 (v/v) acetonitrile/H_2O/formic acid; B, 95/5/0.5 (v/v) acetonitrile/H_2O/formic acid] over 2.5 min was performed for eluting peptides at a flow rate of 300 μL/min. To obtain efficient electrospray ionization, the LC flow was split in a 1/1000 ratio. The LC eluent was then directed to a custom-built Velos Pro 14.5 T Fourier transform ion cyclotron resonance (FT-ICR) mass spectrometer (Thermo Scientific, San Jose, CA).[37] The mass spectra were collected from m/z 400 to 1300 at a high mass resolving power (experimental resolving power $m/\Delta m_{50\%}$ = 100000 at m/z 800, in which $\Delta m_{50\%}$ is the mass spectral peak full width at half-maximum peak height). Proteolysis sequence coverage was insufficient for high spatial resolution by HDX-MS due to the considerable number of large fragments and the lack of common proteolytic peptides between NCAD1 and NCAD12. Structural differences between dimerization interfaces could not be pinpointed, however, proteolysis did provide critical insight into the stable substructures in the Iglike domain, NCAD1 (see below).

RESULTS

Systematic studies of the structure and function of NCAD1 are presented in this work. First, we establish a pathway for the interconversion between monomeric and dimeric forms of NCAD1 and their unique spectroscopic signatures. Second, we assess the kinetics of dimer assembly and disassembly and the dimer dissociation constant by using analytical size-exclusion chromatography (SEC). Finally, we characterize the stability of NCAD1 by using biophysical and proteolytic footprinting.

Reversible Conversion of Monomeric and Dimeric Forms of NCAD1. The monomer and dimer levels in the initial stock immediately following preparation (Figure 2A), dimer and heat-treated monomer stock (Figure 2B), and re-formed dimer stock (Figure 2C) can be seen alongside the experimental design for interconversion of monomeric and dimeric NCAD1 (Figure 2D). The first eluted peak, the larger molecule, represents the level of the dimer. The second peak, the smaller molecule, indicates the level of the monomer. Over time at −20 °C, the NCAD1 initial stock (Figure 2A; 33% D, 67% M) became primarily dimer (dimer stock; Figure 2B, black; 73% D, 27% M). The formation of the dimer was unexpected, because calcium is typically required for dimer formation in N-cadherin. In our NCAD1 construct, the calcium-binding region is incomplete, such that NCAD1 cannot bind calcium under our buffer conditions (1 μM). After heat treatment, the amount of dimer decreased. The resultant NCAD1 solution is the monomer stock (Figure 2B, red; 15% D, 85% M) and indicates that heat reversibly converts the dimer to the monomer, an observation that is further supported by thermal denaturation studies that will be reported below. After incubation over a period of 8 months at 4 °C, the heat-treated monomer stock re-formed the dimer (Figure 2C; 70% D, 30% M).

Spectroscopic Evidence of Structural Differences between the Monomer and Dimer. Asymmetric bonds in proteins absorb left- and right-handed circularly polarized light to different extents. Differences in the CD signal in the region in which the peptide bonds absorb light impart valuable global structural information by probing the general arrangement of the peptide bonds. Figure 3 shows CD spectra of the NCAD1 dimer stock (black), heat-treated monomer stock (red), and re-formed dimer stock (blue). Minima at ∼215 nm are expected from the presence of β-sheets,[38] and the maximum at 230 nm is consistent with the presence of W2.[22] The dimer stock (black) and the re-formed dimer stock (blue) appear identical, consistent with an interpretation that the dimer that re-forms from the heat-treated monomer stock is spectroscopically indistinguishable from the dimer prior to heat treatment. The dimeric stocks have less negative signal than the monomer stock (red), indicating distinctly arranged peptide bonds, pointing to distinct folded structures of the monomer and dimer.

Steady-state fluorescence emission spectroscopy provides insight into the local environment of tryptophan residues in proteins. NCAD1 contains only one tryptophan, W2, which is located on the N-terminal βA-strand. As an essential component in the strand-swapped interface, W2 docks in the partner protomer's hydrophobic pocket in the dimer structure (Figure 1C). Therefore, fluorescence spectra reflect the differences in the docking interactions between W2 and pocket residues, either its own pocket in the monomer or its partner protomer's pocket in the dimer. As seen in Figure 4,

DOI: 10.1021/acs.biochem.8b00733
Biochemistry 2018, 57, 6404−6415

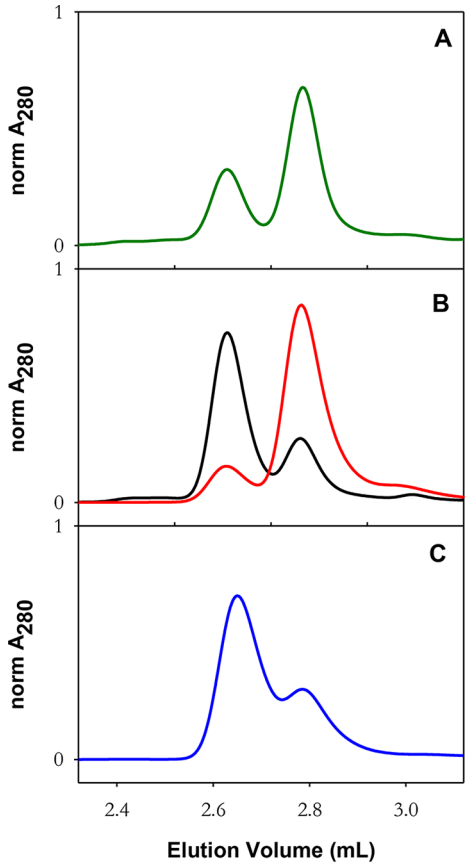

Figure 2. Assessment of monomer–dimer levels of NCAD1 stocks based on analytical SEC: (A) initial stock (green; 33% D, 67% M), (B) dimer stock (black; 73% D, 27% M) and heat-treated monomer stock (red; 15% D, 85% M), and (C) re-formed dimer stock (blue; 70% D, 30% M). All samples injected onto SEC columns (ZORBAX GF-250 and Superose-12 10/300) were analyzed under apo-mobile phase conditions. Elution volumes and total heights were normalized to account for the use of different columns. (D) Experimental design for the preparation of NCAD1 stocks.

the dimer stock (black) and re-formed dimer stock (blue) have emission signals that are stronger than those of the monomer stock (red) for an equivalent protein concentration (2.5 μM). A similar systematic difference is observed for the wavelength of the centroid of the FL emission spectrum between 300 and 410 nm (Table 1); the dimeric structures yield a centroid wavelength that is higher than that of the monomer, indicating that the way in which W2 interacts with hydrophobic pocket residues is distinct in the two structures.

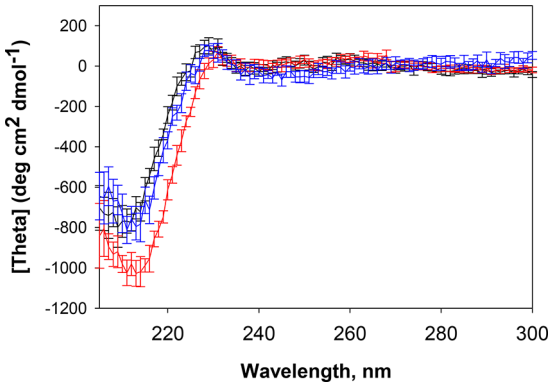

Figure 3. Circular dichroism spectra of NCAD1 stocks. The dimer stock (black; 140 μM), heat-treated monomer stock (red; 140 μM), and re-formed dimer stock (blue; 136 μM) are shown between 210 and 300 nm.

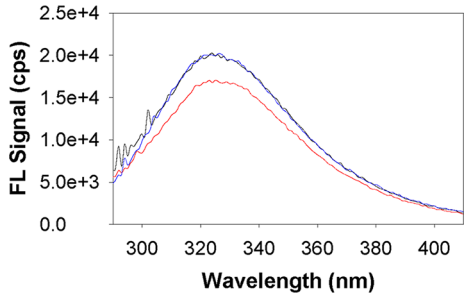

Figure 4. Steady-state fluorescence emission spectra of NCAD1 stocks. The dimer stock (black), heat-treated monomer stock (red), and re-formed dimer stock (blue) are at equivalent protein concentrations (2.5 μM). Excitation at 292 nm.

Table 1. Summary of Relative Maximum and Centroid Wavelengths[a]

stock	centroid (nm)
dimer	337.8
monomer	338.4
re-formed dimer	337.9

[a]The centroid is calculated for the emission between 300 and 410 nm.

Taken together, the data in Figures 3 and 4 indicate that (1) the environments of W2 in the dimer and re-formed dimer stocks are the same, suggesting that the structure of the re-formed dimer is identical to that of the dimer prior to heat treatment, and (2) the environment of W2 in the closed dimer is different from that in the closed monomer.

Equilibrium and Kinetics of Calcium-Independent Dimerization of NCAD1. Both dimer assembly and dimer disassembly experiments were conducted to derive assembly rate, disassembly rate, and equilibrium binding constants.

Assembly Studies. The concentrated dimer stock was heat-treated to create the monomer stock that was diluted, and the re-formation of the dimer was studied over time. To assess the rate of dimer formation, the monomer stock, 140 and 70 μM, was stored at 4 °C, and the level of dimer was assessed as a function of time for a 4 month period by use of analytical SEC. Figure 5A shows representative SEC chromatograms of dimer formation from the 140 μM monomer stock over a period of 126 days. The level of dimer steadily increased from 15 to 70%. Figure 5B illustrates the "hyperbolic" shape of the re-formation

DOI: 10.1021/acs.biochem.8b00733
Biochemistry 2018, 57, 6404–6415

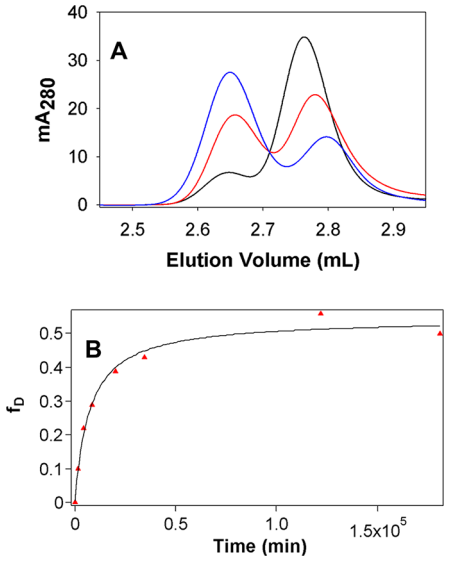

Figure 5. Assembly studies of the NCAD1 dimer. (A) SEC–HPLC data for dimer assembly from the 140 μM NCAD1 monomer. The % D and f_D were calculated for each time point. Chromatograms for 1 h (black), 6 days (red), and 126 days (blue) are shown. (B) The curve is simulated on the basis of a fit of the data to eqs 2 and 3 that resolves an apparent association rate constant and equilibrium dissociation constant as reported in Table 2. Data are shown as red triangles.

profile as a function of incubation period. We fitted these data to a second-order assembly model (eq 2) and obtained a value of 1.2 ± 0.2 M^{-1} min^{-1} for k_f and a value of 120 ± 40 μM for K_d.

Disassembly Studies. The NCAD1 dimer stock was allowed to disassemble over a period of 1 month. Figure 6A shows representative SEC chromatograms over 24 days for 70 μM

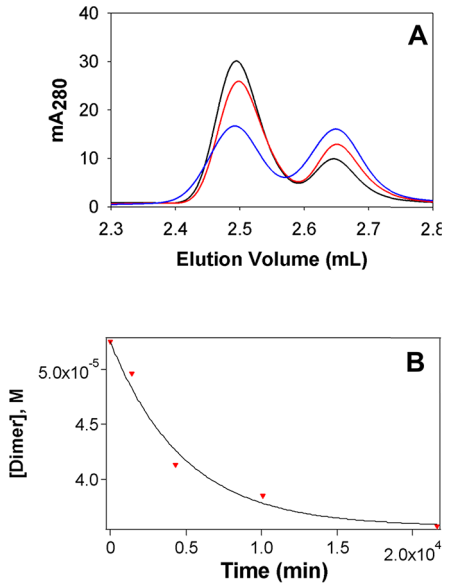

Figure 6. Disassembly of the NCAD1 dimer. (A) SEC–HPLC data for dimer disassembly of the 70 μM dimer stock. Chromatograms for 1 day (black), 2 days (red), and 16 days (blue) are shown. (B) % D and then [dimer] were calculated (red triangles) and plotted vs incubation time. The curve is simulated on the basis of a fit of the data to eq 4. The apparent dissociation rate constant and equilibrium dissociation constant are listed in Table 2.

NCAD1 stored at 4 °C. Over time, the level of the dimer decreases as the level of the monomer increases. The level of the dimer decreased from 75 to 51%. As shown in Figure 6B, the data were fitted to a pseudo-first-order disassembly model (eq 4) to estimate a rate constant of dimer disassembly, k_r, of (2 ± 1) × 10^{-4} min^{-1} and a dissociation equilibrium constant, K_d, of 92 ± 14 μM (Table 2). A value of $t_{1/2}$ was calculated from eq 5 to be 2 days.

Table 2. Resolved Parameters from Analysis of Assembly and Disassembly Studies[a]

experiment	rate constants	equilibrium constant
assembly	k_f = 1.2 ± 0.2 M^{-1} min^{-1}	K_d = 120 ± 40 μM
disassembly	k_r = (2 ± 1) × 10^{-4} min^{-1}	K_d = 92 ± 14 μM
calculated K_d	–	K_d = 166 ± 88 μM[b]

[a]Three independent data sets with two different protein concentrations were simultaneously analyzed to resolve parameters and errors reported for the assembly and disassembly reactions. [b]The value of K_d was calculated from the ratio of the resolved rate constants. The reported error is propagated on the basis of the error in the rate constants.

Stability Studies for the NCAD1 Monomer and Dimer. Thermal denaturations of the NCAD1 stocks were performed to identify differences in stability between the monomeric and dimeric structures. Figure 7 shows the CD-monitored thermal unfolding of NCAD1 stocks at a low protein concentration (5 μM). The dimer (Figure 7A, black) has two transitions. The first corresponds to the disassembly of the dimer at a T_m of 48.6 ± 0.8 °C, as supported by the analytical SEC analysis of the heat-treated monomer stock. The second transition in the dimer stock and the only transition in the monomer stock (Figure 7B; red; T_m of 77.2 ± 0.1 °C) is the unfolding of the EC1 domain. The first and second transitions of both the original NCAD1 stock and the re-formed dimer stock are identical. Data for each transition were fitted to the Gibbs–Helmholtz equation to resolve values for the enthalpy change of unfolding, ΔH_m, and the melting temperature, T_m. The resolved values for ΔH_m and T_m for the unfolding of the EC1 domain in all stocks were very similar, as seen in Table 3. These studies indicate that the dimer and monomer have the same high global stabilities in terms of unfolding the domain itself; EC1 is very stable with a T_m of ~77 °C, a ΔH_m of 84 kcal/mol, and a calculated stability at 25 °C ($\Delta G_{25\ °C}$) of 8.3 kcal/mol.

Analysis of the surface accessibility of amino acid side chains in PDB entry 1NCI indicates that 29 residues with >85% of their side chains are inaccessible to water in the folded structure, comprising a stable hydrophobic core. The atoms of these buried residues are shown in Figure 7D as filled spheres, including those colored red and blue. The subset of the amino acids that were identified as core residues common with TNfn3,[39] and to Ig-like domains, in general,[40,41] is colored blue.

The sequence coverage map for NCAD1 illustrates peptides formed from the proteolysis of the NCAD1 monomer with Protease XIII at pH 2.5 in 8 M urea (Figure 8). The mass range was established from fragments ranging in size from 5 to 45 amino acids. The FT-ICR time domain signal acquisition period was 0.76 s, and the target ion number was set to 3 million by a single fill of ions with automatic gain control before transfer to the ICR cell. The mass spectra were

DOI: 10.1021/acs.biochem.8b00733
Biochemistry 2018, 57, 6404–6415

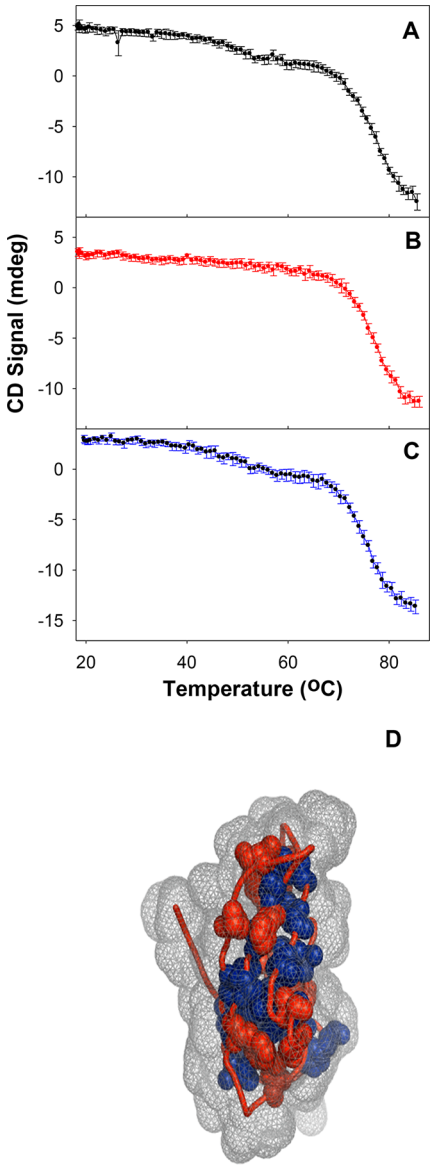

Figure 7. Thermal unfolding of NCAD1 monitored by CD spectroscopy: (A) dimer stock (77% D), (B) heat-treated monomer stock (9% D), and (C) re-formed dimer stock (70% D). All stocks were monitored at 5 μM at a fixed wavelength of 227 nm. (D) Residues with <15% surface exposure are highlighted in NCAD1 (PDB entry 1NCI;[25] PyMol[24]). The exposed surface of the protein is represented as a wire frame.

Table 3. Summary of Resolved Parameters from Thermal Unfolding Experiments with NCAD1[a]

stock	ΔH_m (kcal/mol)	T_m (°C)	$\Delta G_{25\ °C}$ (kcal/mol)
dimer			
transition 1	35 ± 6	48.6 ± 0.8	1.7 ± 0.9
transition 2	76 ± 2	77.1 ± 0.1	7.2 ± 0.3
monomer	85 ± 2	77.2 ± 0.1	8.5 ± 0.3
re-formed dimer			
transition 1	34 ± 9	49 ± 2	1.6 ± 0.4
transition 2	90 ± 4	75.6 ± 0.1	9.2 ± 0.4

[a]The value of ΔC_p was fixed at 1 kcal mol^{-1} K^{-1}. $\Delta G_{25\ °C}$ is the calculated value of the free energy change upon unfolding at 25 °C.

externally calibrated with peptide standards; thus, the mass errors are typically <1 ppm. Mass spectra in magnitude mode were collected with Xalibur (Thermo Scientific, San Jose, CA), and peptides were identified on the basis of accurate masses by custom software.[42] Ambiguities in identification were resolved by considering the cleavage preferences of Protease XIII.[43]

Starting from the N-terminus, fragments for the first ~25 amino acids indicate that this region is readily proteolyzed into small fragments, averaging 13 residues in length, shorter than those for the rest of the sequence. The overall sequence coverage map reveals a high number of large fragments, averaging 28 amino acids in length, from approximately K30 to approximately E69, a region that includes the βC-strand (L34−T39), the βD-strand (F51−I53), and the βE-strand (Q59−V62). This proteolysis-resistant region (approximately K30 to approximately E69) contains 52% of the hydrophobic core residues identified from side chain accessibility to solvent, and it is represented in the ribbon drawing in Figure 9. We expected the long C−D loop region (G40−I50) to be susceptible to proteolysis because of solvent accessibility; however, amino acids in this region have a poor cleavage preference by Protease XIII, and the sequence contains amino acids considered to be contributors to the hydrophobic core (A43 and I50), as well as P46P47, which would serve to rigidify the segment. As for the N-terminal region, the C-terminal segment (L70−I99) is readily proteolyzed into fragments smaller than those for the proteolysis-resistant region. The fragments are smaller in the C-terminal segment, averaging 15 residues in length, which includes the βF- and βG-strands. Because the peptides from this region are primarily cleaved from both termini, it appears that the βF- and βG-strands may remain hydrogen-bonded to the βC-, βD-, and βE-strand core region and that they are degraded from the termini as digestion proceeds. This idea is supported by the finding that 38% of the amino acids comprising the βF- and βG-strands and the intervening loop contribute to the hydrophobic core.

Taken together, stability studies of the NCAD1 monomer and dimer point to an exceptionally high intrinsic stability for an isolated domain with no internal disulfides. Thermal denaturation studies show that the high stability is independent of the dimerization state. Moreover, analysis of the surface accessibility of amino acids in PDB entry 1NCI indicates a stable hydrophobic core larger than that of TNfn3 and Ig-like domains in general. Proteolytic mapping of the NCAD1 monomer further points to a proteolysis-resistant region containing the βC-strand (L34−T39), the βD-strand (F51−I53), and the βE-strand (Q59−V62).

DISCUSSION

N-cadherin has a vital role in numerous developmental processes, as is evident from regulation of its expression levels as a function of the maturation of tissues, such as vasculature,[15] and in the formation of the neural tube during development.[44] As the signature molecule for long-term potentiation,[45] N-cadherin stabilizes excitatory synapses[46] but allows for the necessary plasticity of their footprint.[46,47] These temporal and tissue-specific roles indicate that N-cadherin must be more suitable for such venues than E-cadherin, the classical cadherin involved in stable adherens junctions found primarily in epithelial tissues. They differ in their dimerization affinity but most notably in their calcium-dependent kinetics of dimerization. Hence, we have an abiding interest in the molecular

DOI: 10.1021/acs.biochem.8b00733
Biochemistry 2018, 57, 6404−6415

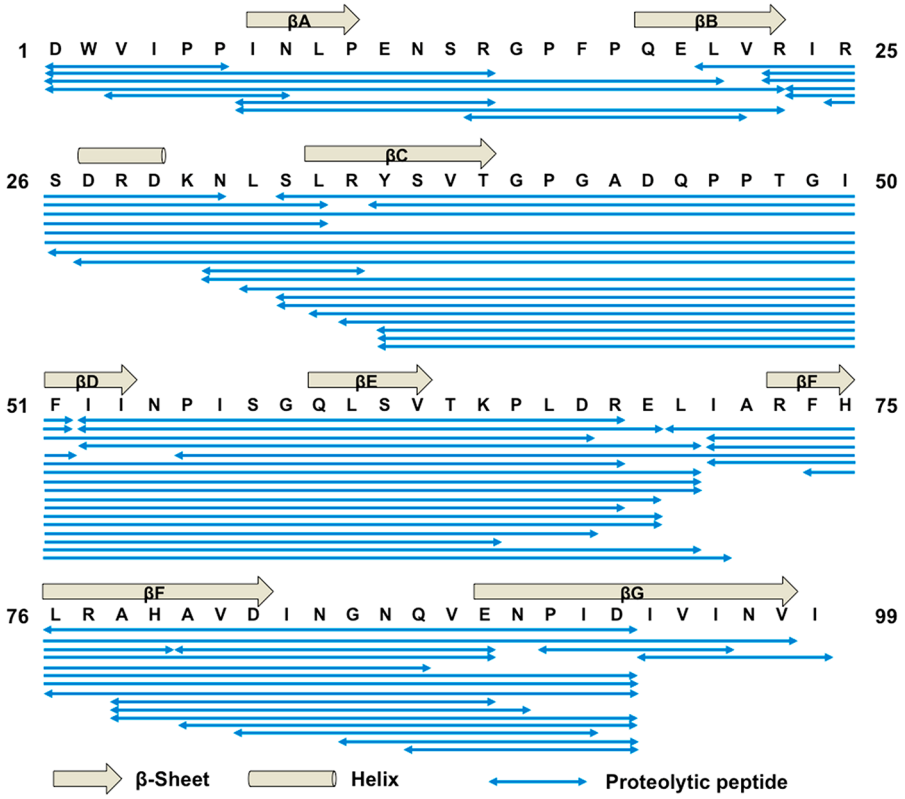

Figure 8. Sequence coverage map of the NCAD1 monomeric stock by Protease XIII. Blue arrow bars below the primary sequence of NCAD1 denote proteolytic peptide coverage from the digestion experiment. The secondary structure above the sequence represents the βA–βG-strands throughout the sequence.

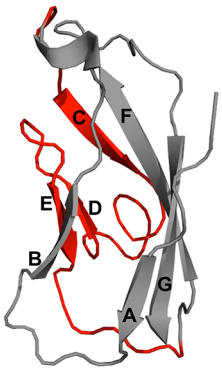

Figure 9. Ribbon drawing of NCAD1 representing the proteolysis-resistant region of NCAD1 (PDB entry 1NCI;[25] PyMol[24]). Residues 30–69 are colored red to indicate the region identified by high-resolution peptide mapping as the most resistant to proteolysis. β-Sheets A–G are labeled.

determinants that distinguish N- and E-cadherins. It is interesting to note that the specific residues known to be critical for dimerization and calcium binding are identical in the two proteins and are, therefore, not the origin of the difference in their dimerization kinetics. Thus, although there must be an "initial encounter complex" in N-cadherin, the structural basis for it is ambiguous.[30,48,49] Adhesive interactions mediated by E- and N-cadherin involve the direct interaction of the most distal modular extracellular domain, EC1, through a strand-swapped structure involving insertion of W2 into a hydrophobic pocket on the adhesive partner. Here, we present studies of the biophysical properties of NCAD1 that elucidate its role in adhesion. Our studies indicate that the monomer–dimer equilibrium is spontaneous and reversible, but both assembly and disassembly are slow. Below we discuss our data in the larger context of protein folding and function.

Disposition of the βA-Strand and Dimerization Affinity. NCAD1 has the unusual property of forming a dimeric structure that is not driven by calcium binding. NCAD1 spontaneously forms a dimer over time even in frozen stock solutions. Evidently, the protein is concentrated as ice crystals lead to concentration of the protein. However, the monomer formed after heat treatment of the dimer-enriched stocks subsequently re-formed the dimer as a function of the K_d of dimerization and protein concentration.

Our spectroscopic and thermal denaturation data indicate that the dimer in our initial stock solutions and the dimer that re-formed from the heat-treated monomer stock are similar in structure and stability. The emission maximum is ~324 nm, indicating that W2 is protected from the aqueous solvent and that it is equally buried in the monomeric and dimeric forms. The difference in the intensity of the fluorescence emission signals between the monomer and dimer is consistent with an intrinsic difference in the interaction of W2 with the residues in the hydrophobic pocket. This interaction has been studied by several groups in NCAD12, the EC1–linker 1–EC2–linker 2 construct, based on mutations of residues in the hydrophobic pocket. Vendome et al. created the A78S/I92M mutant, effectively changing the hydrophobic pocket residues in NCAD12 to those of ECAD12 (NCAD:NtoE).[48] One would anticipate that this mutation would decrease the dimerization affinity of NCAD12 ($K_d = 2.5 \times 10^{-5}$) to be more similar to that of ECAD12 ($K_d = 10 \times 10^{-5}$). However, these mutations

DOI: 10.1021/acs.biochem.8b00733
Biochemistry 2018, 57, 6404–6415

caused the dimerization affinity of NCAD:NtoE to increase, contrary to anticipated results.[48] It is clear that the hydrophobic pocket residues impact the affinity of dimerization, although the W2−hydrophobic pocket interaction is not the only factor involved in dictating NCAD12 affinity. Similar results were found in an antibody binding assay performed by Harrison et al. in 2005.[50,51]

It is known that binding of calcium to NCAD12 induces strain in the closed monomer that is released upon formation of the strand-swapped dimer;[22] yet this scenario cannot be applied to NCAD1 because it forms a dimer without calcium binding. The parallel argument for the NCAD1 monomer is that the closed monomeric form is intrinsically strained, but the energy of hydration of a solvent-exposed indole ring exceeds the energy of the interaction of W2 with the hydrophobic pocket residues. Formation of the dimer relieves the strain in the NCAD1 closed monomer. It seems that the strain is not in the hydrophobic core of NCAD1 because the dimer and monomer have identical denaturation profiles. Instead, the driving force of dimerization in NCAD1 seems to be isolated to the βA-strand in the closed monomer, directing our attention to the W2−hydrophobic pocket interaction. NCAD1 has the same noncovalent forces (docked W2 and ionic interaction between E89 and the N-terminus) in both the monomeric and dimeric forms; yet the interaction between W2 and the residues in the hydrophobic pocket appears to be distinct.

Further evidence that supports the idea that the W2−hydrophobic pocket interaction is a key factor in dimerization affinity comes from computational and structural studies of the relative disposition of the EC1 domains in strand-swapped structures in classical cadherins. We are confident that the first crystallographic structure of NCAD1 [PDB entry 1NCI (Figure 1B)] is the exact dimeric structure we studied here: both dimer and re-formed dimer stocks that have indistinguishable structures. The disposition of EC1 in the 1NCI crystal structure is different than that seen in strand-swapped structures of the EC1−linker 1−EC2 constructs of NCAD and ECAD, wild-type and mutant proteins as reported by Vendome et al.[48] Considering computational work, Cailliez et al. studied the relative orientation of E-cadherin and found two minima in the angle between protomers in strand-swapped structures.[52] Calculation of the relative energies of those orientations indicated that both states would be populated in the absence of stabilizing interactions found in vivo and in a crystal lattice. Recently, a computational structure was determined for ECAD that is a strand-swapped structure, but a larger EC1−EC1 buried surface area with splayed EC2 domains appropriately termed the Y-dimer.[53] Taken together, these studies support the observation that docking of W2 in the hydrophobic pocket and other interactions between the EC1 domains at the strand-swapped interface can explain differences in affinity and energetic driving forces for dimerization in the absence of calcium binding.

Equilibrium and Kinetics of Dimerization. We are able to study the equilibrium and kinetics of NCAD1 by using a simple chromatographic assay because of the extraordinarily slow kinetics of disassembly of the NCAD1 dimer. Systematic studies of the kinetics of assembly of the monomer and disassembly of the dimer provide both kinetic constants and the equilibrium constant. The plateau in both studies yields estimates of the K_d for dimerization, a value of ∼150 μM. It is worth noting that this value is a relatively high dimerization affinity for classical cadherins, with a K_d on the order of the calcium-induced dimer assembly of ECAD12 (K_d = 100 μM), and ∼1/6 of the affinity of the calcium-dependent NCAD12 dimer (K_d = 25 μM).[28,48] Furthermore, the K_d was also calculated simply from the ratio of forward and reverse rate constants and found to agree with the value recovered from the plateau values, consistent with the interpretation that the dimerization process is a two-state process (2M ↔ D).

The assembly and disassembly of the NCAD1 dimer are both very slow, with a $t_{1/2}$ for disassembly of 2 days, and the assembly constant is 4 orders of magnitude smaller than is typical for a bimolecular reaction typical for protein association.[54] Although the equilibrium constant is on the same order of magnitude as that for ECAD12 and NCAD12, our data support the idea that there is a significant activation energy barrier between monomeric and dimeric forms. Temperature-dependent studies were compromised by the tendency for the NCAD1 monomer to adsorb to the SEC column at the long incubation periods required for disassembly at temperatures of >4 °C. Because the kinetics are very slow even at higher temperatures [τ ∼ 1 day at 25 °C (data not shown)], we could not acquire meaningful temperature-dependent data.

The formation of strand-swapped dimers requires a very specific orientation of protomers and the opening of the βA-strands so that they can dock in the partner protomer. This complex requirement for dimerization is well modeled by an initial encounter dimer, in the E-cadherin two-domain constructs, that effectively lowers the activation energy barrier for strand swapping between protomers. The existence of this low-affinity, transient complex has been supported by X-ray crystallographic,[48] sedimentation equilibrium,[48] and bioforce probe[55] experiments and involves interactions between residues in EC1 of one protomer and EC2 residues of the partner protomer. On the basis of this model, for our studies of NCAD1, we would expect that the assembly and disassembly of dimer would be slow because the initial encounter complex would not form and the transition state between the monomer and dimer would not be stabilized.

Intrinsic Stability of NCAD1. Stability studies of the isolated modular domains of E- and N-cadherins show exceptional stability for ∼100-residue proteins with no internal disulfides.[35,40] Analysis of thermal stabilities of the dimeric and monomeric stocks of NCAD1 presented here yielded an average T_m of 77 °C and a ΔH_m of 84 kcal/mol (calculated stability $\Delta G_{25\ °C}$ = 8.3 kcal/mol). These values indicate a stability significantly greater than that of isolated EC2 constructs with or without the adjoining linker segments.[35,56] Moreover, the stability of NCAD1 is unaffected by the presence of either 1 mM calcium or 1 M NaCl (data not shown), indicating that electrostatic interactions neither stabilize nor destabilize the core NCAD1 structure, directing attention to the hydrophobic core of the protein as the source of this remarkable stability.

The absence of a difference in the intrinsic stability of the NCAD1 monomeric and dimeric forms is an important observation. Taken together with the spectroscopic data, this result has two possible interpretations: W2 docked in the hydrophobic pocket either stabilizes both structures equally or has no effect on the intrinsic stability of NCAD1. When the dimer disassembles at 50 °C, it is possible that W2 is exposed and then docked into the hydrophobic pocket of its own subunit. Our studies cannot address this issue directly because

DOI: 10.1021/acs.biochem.8b00733
Biochemistry 2018, 57, 6404−6415

of the strong temperature dependence of fluorescence emission.[57] However, studies of the W2A and E89A mutants of NCAD12 indicated that there is no CD signal from the unfolding of EC1 in the two-domain construct if W2 is absent (W2A mutant) or incompletely docked in the hydrophobic pocket (E89A mutant), consistent with our interpretation that W2 is docked in NCAD1 after the dimer is disassembled at 50 °C.[22]

Evaluation of proteolytic peptides from digestion of the NCAD1 monomer measured with high-resolution mass spectrometry yielded important information about the integrity of the domain. Although NCAD1 monomer fragments spanned the entire sequence, large fragment sizes would result in inadequate site-specific HDX-MS data. There is an overall low level of cleavage at pH 2.5 in 8 M urea, indicating that NCAD1 is folded, even under these extreme conditions. Steady-state fluorescence emission spectra indicate that the tryptophan in NCAD1 is not completely exposed in 8 M dimethylurea, a denaturant that is stronger than urea (SI Figure 1). Moreover, in separate experiments with NCAD12, proteolysis of EC1 yielded more and larger fragments than EC2, which was degraded into small fragments, averaging 10 residues in length (manuscript in preparation). These peptide mapping experiments are consistent with stability studies of the individual domains: NCAD1 studies reported here and NCAD2 studies reported elsewhere.[35,56] Proteolytic mapping of the NCAD1 monomer points to a proteolysis-resistant region containing β-sheets C−E (L34−V62) that is protected from cleavage and undergoes little fragmentation with Protease XIII. This apparently stable core structure comprised of approximately residues 30−69 is a region within this Ig-like domain similar to the stable core identified by Hamill et al.[39] It is important to note that the stability of NCAD1 is insensitive to 1 M NaCl (SI Figure 2), and therefore, we argue that these findings from proteolysis at pH 2.5 are indicative of the folded structure at pH 7.

Ig-like domains are a sandwich of two multistrand sheets (B−E−D β-sheets and C−F−G−A β-sheets). The C−D−E region spans the sandwich and is likely the intermediate on the folding pathway that both stabilizes the global fold and nucleates the rapid kinetics of folding.[40] In contrast to Hamill et al.,[39] our βB-strand is degraded by protease, indicating that it is labile and not a significant contributor to the stabilization of the transition state.[39] In studies of TNfn3, the βF- and βG-strands do not play a role in stabilization of the transition state between the folded and unfolded states.[39] However, considering the residues contributing to the global stability of the folded state, we predict that the βF- and βG-strands are significant contributors in NCAD1. These data, taken together, are consistent with the literature but indicate that NCAD1 is very stable for an Ig-like domain.

Relevance to Physiology. Although calcium levels in vivo are considered to be ∼1 mM, at the extreme conditions at an excitatory synapse they can decrease to far lower levels. In the diffusion-restricted space surrounding excitatory synapses,[58] calcium levels have been measured to be as low as 100 μM[59] and 40 μM,[60] and these authors note that the levels may drop significantly more in the synaptic cleft. As such, characterizing the kinetics and equilibria of calcium dependent-cell adhesion is critical to understanding synapse dynamics. We consider NCAD1 as the minimal subunit that forms the dimer in the absence of calcium. The slow kinetics reported for dimer disassembly of NCAD1 (τ = 2 days; K_d = 130 μM) represent the slowest event that we would predict at an excitatory synapse. In contrast, at the other end of the scale, we find that NCAD12, with an intact calcium binding pocket, has a τ value of 15 s and a K_d for dimerization of 25 μM in 1 mM calcium.[49] As such, the studies reported here on a simplified protein construct predict limiting values for synapse plasticity in vivo.

CONCLUSION

As the transmembrane component of adherens junctions, cadherins are vital in linking the actin cytoskeletons of proximal cells. Previous collective studies of modular EC domains have pointed to the essential adhesive role and the remarkable stability of the EC1 domain, and studies reported here investigated this most distal 99-amino acid, Ig-like domain of N-cadherin. Diverse dimerization affinities among classical cadherin family members are conserved throughout evolution because of their critical effects on cells' adhesive behaviors. NCAD1's unique ability to spontaneously form a dimer without calcium binding implies cooperativity between the modular extracellular domains that directly influences kinetics and equilibria unique to N-cadherin. We presented results of systematic studies of the structure and function of NCAD1. Spectroscopic studies show that W2 remains docked in the both monomeric and dimeric forms yet has a different disposition within the hydrophobic pockets. Thermal denaturation studies show the monomer and dimer have equivalent and exceptionally high intrinsic stability. Combined with our work on the equilibrium and kinetics of the unexpected dimerization phenomenon, we believe that the dimerization driving force does not originate from the hydrophobic core but originates from the βA-strand, specifically the W2−hydrophobic pocket interaction. The assembly and disassembly are exceptionally slow, although the equilibrium constant is on the same order of magnitude as for calcium-saturated NCAD12 and ECAD12. We conclude that NCAD1 is missing critical contacts that stabilize the initial encounter complex that facilitates the exchange of the βA-strand in NCAD12, and therefore, NCAD1 forms significant levels of only the slow-exchange dimer. Considering that N-cadherin is a protein that is required at excitatory synapses, the site of long-term potentiation, its ability to adapt the kinetics and equilibria of adhesive dimerization in response to low calcium concentrations is obligatory.

ASSOCIATED CONTENT

Supporting Information

The Supporting Information is available free of charge on the ACS Publications website at DOI: 10.1021/acs.biochem.8b00733.

Chemical denaturation of NCAD1 (SI Figure 1) and thermal denaturation of NCAD1 in 1 M NaCl (SI Figure 2) (PDF)

AUTHOR INFORMATION

Corresponding Author

*Address: 122 Coulter Hall, Department of Chemistry and Biochemistry, University of Mississippi, University, MS 38677. E-mail: spedigo@olemiss.edu. Phone: 1-662-915-7561. Fax: 1-662-915-7300.

ORCID

Samantha Davila: 0000-0001-9263-1536

Peilu Liu: 0000-0002-0467-303X

DOI: 10.1021/acs.biochem.8b00733
Biochemistry 2018, 57, 6404−6415

Alan G. Marshall: 0000-0001-9375-2532

Present Address

[‖]A.S.: Biomedical Sciences, University of Kentucky, Lexington, KY 40506.

Funding

This work was supported in part by GAANN Award P200A1200 through the Department of Education. A portion of this work was performed at the National High Magnetic Field Laboratory, which is supported by National Science Foundation Cooperative Agreement DMR-1157490 and the State of Florida.

Notes

The authors declare no competing financial interest.

■ ABBREVIATIONS

apo, calcium-free; CD, circular dichroism; EC, extracellular domain; EC1, extracellular domain 1 of NCAD12; EC2, extracellular domain 2 of NCAD12; ECAD12, epithelial cadherin domains 1 and 2; EDTA, ethylenediaminetetraacetic acid; FL, fluorescence emission; HDX-MS, hydrogen/deuterium-exchange mass spectrometry; HEPES, N-(2-hydroxyethyl)piperazine-N0-2-ethanesulfonic acid; K_d, dissociation constant; NCAD12, neural cadherin domains 1 and 2 (residues 1−221); PDB, Protein Data Bank; SEC, size-exclusion chromatography; T_m, melting temperature; WT, wild-type NCAD12; FT-ICR, Fourier transform ion cyclotron resonance.

■ REFERENCES

(1) Angst, B. D., Marcozzi, C., and Magee, A. I. (2001) The cadherin superfamily: diversity in form and function. *J. Cell Sci. 114*, 629−641.

(2) Leckband, D., and Sivasankar, S. (2012) Cadherin recognition and adhesion. *Curr. Opin. Cell Biol. 24*, 620−627.

(3) Takeichi, M. (1990) Cadherins: a molecular family important in selective cell-cell adhesion. *Annu. Rev. Biochem. 59*, 237−252.

(4) Benson, D. L., and Tanaka, H. (1998) N-cadherin redistribution during synaptogenesis in hippocampal neurons. *J. Neurosci. 18*, 6892−6904.

(5) Shapiro, L., Love, J., and Colman, D. R. (2007) Adhesion molecules in the nervous system: structural insights into function and diversity. *Annu. Rev. Neurosci. 30*, 451−474.

(6) Yu, X., and Malenka, R. C. (2004) Multiple functions for the cadherin/catenin complex during neuronal development. *Neuropharmacology 47*, 779−786.

(7) Jungling, K., Eulenburg, V., Moore, R., Kemler, R., Lessmann, V., and Gottmann, K. (2006) N-cadherin transsynaptically regulates short-term plasticity at glutamatergic synapses in embryonic stem cell-derived neurons. *J. Neurosci. 26*, 6968−6978.

(8) Huntley, G. W., Gil, O., and Bozdagi, O. (2002) The cadherin family of cell adhesion molecules: multiple roles in synaptic plasticity. *Neuroscientist 8*, 221−233.

(9) Redies, C. (2000) Cadherins in the central nervous system. *Prog. Neurobiol. 61*, 611−648.

(10) Hirano, S., Suzuki, S. T., and Redies, C. (2003) The cadherin superfamily in neural development: diversity, function and interaction with other molecules. *Front. Biosci., Landmark Ed. 8*, d306−356.

(11) Bozdagi, O., Shan, W., Tanaka, H., Benson, D. L., and Huntley, G. W. (2000) Increasing numbers of synaptic puncta during late-phase LTP: N-cadherin is synthesized, recruited to synaptic sites, and required for potentiation. *Neuron 28*, 245−259.

(12) Fannon, A. M., and Colman, D. R. (1996) A model for central synaptic junctional complex formation based on the differential adhesive specificities of the cadherins. *Neuron 17*, 423−434.

(13) Manabe, T., Togashi, H., Uchida, N., Suzuki, S. C., Hayakawa, Y., Yamamoto, M., Yoda, H., Miyakawa, T., Takeichi, M., and Chisaka, O. (2000) Loss of cadherin-11 adhesion receptor enhances plastic changes in hippocampal synapses and modifies behavioral responses. *Mol. Cell. Neurosci. 15*, 534−546.

(14) Giampietro, C., Taddei, A., Corada, M., Sarra-Ferraris, G. M., Alcalay, M., Cavallaro, U., Orsenigo, F., Lampugnani, M. G., and Dejana, E. (2012) Overlapping and divergent signaling pathways of N-cadherin and VE-cadherin in endothelial cells. *Blood 119*, 2159−2170.

(15) Luo, Y., and Radice, G. L. (2005) N-cadherin acts upstream of VE-cadherin in controlling vascular morphogenesis. *J. Cell Biol. 169*, 29−34.

(16) Hazan, R. B., Qiao, R., Keren, R., Badano, I., and Suyama, K. (2004) Cadherin switch in tumor progression. *Ann. N. Y. Acad. Sci. 1014*, 155−163.

(17) Mariotti, A., Perotti, A., Sessa, C., and Rüegg, C. (2007) N-cadherin as a therapeutic target in cancer. *Expert Opin. Invest. Drugs 16*, 451−465.

(18) Ozawa, M., Engel, J., and Kemler, R. (1990) Single amino acid substitutions in one Ca2+ binding site of uvomorulin abolish the adhesive function. *Cell 63*, 1033−1038.

(19) Prakasam, A., Chien, Y. H., Maruthamuthu, V., and Leckband, D. E. (2006) Calcium site mutations in cadherin: impact on adhesion and evidence of cooperativity. *Biochemistry 45*, 6930−6939.

(20) Sivasankar, S., Zhang, Y., Nelson, W. J., and Chu, S. (2009) Characterizing the initial encounter complex in cadherin adhesion. *Structure 17*, 1075−1081.

(21) Chitaev, N. A., and Troyanovsky, S. M. (1998) Adhesive but not lateral E-cadherin complexes require calcium and catenins for their formation. *J. Cell Biol. 142*, 837−846.

(22) Vunnam, N., and Pedigo, S. (2011) Calcium-induced strain in the monomer promotes dimerization in neural cadherin. *Biochemistry 50*, 8437−8444.

(23) Katsamba, P., Carroll, K., Ahlsen, G., Bahna, F., Vendome, J., Posy, S., Rajebhosale, M., Price, S., Jessell, T. M., Ben-Shaul, A., Shapiro, L., and Honig, B. H. (2009) Linking molecular affinity and cellular specificity in cadherin-mediated adhesion. *Proc. Natl. Acad. Sci. U. S. A. 106*, 11594−11599.

(24) *The PyMOL Molecular Graphics System*, version 1.3r1 (2010) Schrodinger, LLC (www.pymol.org).

(25) Shapiro, L., Fannon, A. M., Kwong, P. D., Thompson, A., Lehmann, M. S., Grubel, G., Legrand, J. F., Als-Nielsen, J., Colman, D. R., and Hendrickson, W. A. (1995) Structural basis of cell-cell adhesion by cadherins. *Nature 374*, 327−337.

(26) Tamura, K., Shan, W. S., Hendrickson, W. A., Colman, D. R., and Shapiro, L. (1998) Structure-function analysis of cell adhesion by neural (N-) cadherin. *Neuron 20*, 1153−1163.

(27) Klingelhofer, J., Laur, O. Y., Troyanovsky, R. B., and Troyanovsky, S. M. (2002) Dynamic interplay between adhesive and lateral E-cadherin dimers. *Mol. Cell. Biol. 22*, 7449−7458.

(28) Vunnam, N., Flint, J., Balbo, A., Schuck, P., and Pedigo, S. (2011) Dimeric States of Neural- and Epithelial-Cadherins are Distinguished by the Rate of Disassembly. *Biochemistry 50*, 2951−2961.

(29) Harrison, O. J., Bahna, F., Katsamba, P. S., Jin, X., Brasch, J., Vendome, J., Ahlsen, G., Carroll, K. J., Price, S. R., Honig, B., and Shapiro, L. (2010) Two-step adhesive binding by classical cadherins. *Nat. Struct. Mol. Biol. 17*, 348−357.

(30) Vunnam, N., and Pedigo, S. (2012) X-interface is not the explanation for the slow disassembly of N-cadherin dimers in the apo state. *Protein Sci. 21*, 1006−1014.

(31) Jungles, J. M., Dukes, M. P., Vunnam, N., and Pedigo, S. (2014) Impact of pH on the Structure and Function of Neural Cadherin. *Biochemistry 53*, 7436−7444.

(32) Pace, C. N., Vajdos, F., Fee, L., Grimsley, G., and Gray, T. (1995) How to measure and predict the molar extinction coefficient of a protein. *Protein Sci. 4*, 2411−2423.

(33) Vunnam, N., and Pedigo, S. (2011) Sequential binding of calcium leads to dimerization in neural cadherin. *Biochemistry 50*, 2973−2982.

DOI: 10.1021/acs.biochem.8b00733
Biochemistry 2018, 57, 6404−6415

(34) Greenfield, N., and Fasman, G. D. (1969) Computed circular dichroism spectra for the evaluation of protein conformation. *Biochemistry 8*, 4108−4116.
(35) Prasad, A., Housley, N. A., and Pedigo, S. (2004) Thermodynamic stability of domain 2 of epithelial cadherin. *Biochemistry 43*, 8055−8066.
(36) Fraczkiewicz, R., and Braun, W. (1998) Exact and efficient calculation of the accessible surface areas and their gradients for macromolecules. *J. Comput. Chem. 19*, 319−333.
(37) Schaub, T. M., Hendrickson, C. L., Horning, S., Quinn, J. P., Senko, M. W., and Marshall, A. G. (2008) High-Performance Mass Spectrometry: Fourier Transform Ion Cyclotron Resonance at 14.5 T. *Anal. Chem. 80*, 3985−3990.
(38) Greenfield, N. J., and Fasman, G. D. (1969) Computed circular dischroism spectra for protein conformation. *Biochemistry 8*, 4108−4116.
(39) Hamill, S. J., Steward, A., and Clarke, J. (2000) The folding of an immunoglobulin-like Greek key protein is defined by a common-core nucleus and regions constrained by topology. *J. Mol. Biol. 297*, 165−178.
(40) Clarke, J., Cota, E., Fowler, S. B., and Hamill, S. J. (1999) Folding studies of immunoglobulin-like beta-sandwich proteins suggest that they share a common folding pathway. *Structure 7*, 1145−1153.
(41) Fowler, S. B., and Clarke, J. (2001) Mapping the folding pathway of an immunoglobulin domain: structural detail from Phi value analysis and movement of the transition state. *Structure 9*, 355−366.
(42) Kazazic, S., Zhang, H.-M., Schaub, T., Emmett, M., Hendrickson, C., Blakney, G., and Marshall, A. (2010) Automated Data Reduction for Hydrogen/Deuterium Exchange Experiments, Enabled by High-Resolution Fourier Transform Ion Cyclotron Resonance Mass Spectrometry. *J. Am. Soc. Mass Spectrom. 21*, 550−558.
(43) Zhang, H. M., Kazazic, S., Schaub, T. M., Tipton, J. D., Emmett, M. R., and Marshall, A. G. (2008) Enhanced Digestion Efficiency, Peptide Ionization Efficiency, and Sequence Resolution for Protein Hydrogen/Deuterium Exchange Monitored by Fourier Transform Ion Cyclotron Resonance Mass Spectrometry. *Anal. Chem. 80*, 9034−9041.
(44) Bronner-Fraser, M., Wolf, J. J., and Murray, B. A. (1992) Effects of antibodies against N-cadherin and N-CAM on the cranial neural crest and neural tube. *Dev. Biol. 153*, 291−301.
(45) Bozdagi, O., Wang, X. B., Nikitczuk, J. S., Anderson, T. R., Bloss, E. B., Radice, G. L., Zhou, Q., Benson, D. L., and Huntley, G. W. (2010) Persistence of coordinated long-term potentiation and dendritic spine enlargement at mature hippocampal CA1 synapses requires N-cadherin. *J. Neurosci. 30*, 9984−9989.
(46) Mysore, S. P., Tai, C. Y., and Schuman, E. M. (2008) N-cadherin, spine dynamics, and synaptic function. *Front. Neurosci. 2*, 168−175.
(47) Mendez, P., De Roo, M., Poglia, L., Klauser, P., and Muller, D. (2010) N-cadherin mediates plasticity-induced long-term spine stabilization. *J. Cell Biol. 189*, 589−600.
(48) Vendome, J., Felsovalyi, K., Song, H., Yang, Z., Jin, X., Brasch, J., Harrison, O. J., Ahlsen, G., Bahna, F., Kaczynska, A., Katsamba, P. S., Edmond, D., Hubbell, W. L., Shapiro, L., and Honig, B. (2014) Structural and energetic determinants of adhesive binding specificity in type I cadherins. *Proc. Natl. Acad. Sci. U. S. A. 111*, E4175−4184.
(49) Vunnam, N., Hammer, N. I., and Pedigo, S. (2015) Basic residue at position 14 is not required for fast assembly and disassembly kinetics in neural cadherin. *Biochemistry 54*, 836−843.
(50) Harrison, O. J., Corps, E. M., Berge, T., and Kilshaw, P. J. (2005) The mechanism of cell adhesion by classical cadherins: the role of domain 1. *J. Cell Sci. 118*, 711−721.
(51) Harrison, O. J., Corps, E. M., and Kilshaw, P. J. (2005) Cadherin adhesion depends on a salt bridge at the N-terminus. *J. Cell Sci. 118*, 4123−4130.
(52) Cailliez, F., and Lavery, R. (2006) Dynamics and stability of E-cadherin dimers. *Biophys. J. 91*, 3964−3971.
(53) Schumann-Gillett, A., Mark, A. E., Deplazes, E., and O'Mara, M. L. (2018) A potential new, stable state of the E-cadherin strand-swapped dimer in solution. *Eur. Biophys. J. 47*, 59−67.
(54) Pollard, T. D., and De La Cruz, E. M. (2013) Take advantage of time in your experiments: a guide to simple, informative kinetics assays. *Mol. Biol. Cell 24*, 1103−1110.
(55) Rakshit, S., Zhang, Y., Manibog, K., Shafraz, O., and Sivasankar, S. (2012) Ideal, catch, and slip bonds in cadherin adhesion. *Proc. Natl. Acad. Sci. U. S. A. 109*, 18815−18820.
(56) Prasad, A., Zhao, H., Rutherford, J. M., Housley, N. A., Nichols, C., and Pedigo, S. (2006) Effect of linker segments upon the stability of Epithelial-Cadherin Domain 2. *Proteins: Struct., Funct., Genet. 62*, 111−121.
(57) Eftink, M. R., Gryczynski, I., Wiczk, W., Laczko, G., and Lakowicz, J. R. (1991) Effects of temperature on the fluorescence intensity and anisotropy decays of staphylococcal nuclease and the less stable nuclease-conA- SG28 mutant. *Biochemistry 30*, 8945−8953.
(58) Sykova, E., and Nicholson, C. (2008) Diffusion in Brain and Extracellular Space. *Physiol. Rev. 88*, 1277−1340.
(59) Hofer, A. M. (2005) Another dimension to calcium signaling: a look at extracellular calcium. *J. Cell Sci. 118*, 855−862.
(60) Rusakov, D. A., and Fine, A. (2003) Extracellular Ca2+ depletion contributes to fast activity-dependent modulation of synaptic transmission in the brain. *Neuron 37*, 287−297.

DOI: 10.1021/acs.biochem.8b00733
Biochemistry 2018, 57, 6404−6415